Stochastic Environmental Research and Risk Assessment
https://doi.org/10.1007/s00477-022-02335-7

ORIGINAL PAPER

Extreme wind speed prediction in mountainous area with mixed wind climates

Teng Ma[1] · Wei Cui[1,2] · Lin Zhao[1,2] · Ding Yejun[1] · Fang Genshen[1,2] · Yaojun Ge[1,2]

Accepted: 11 October 2022

Abstract

In addition to common synoptic wind system, the mountainous terrain forms a local thermally driven wind system, which makes the mountain wind system have strong terrain dependence. Therefore, in order to estimate the reliable design wind speeds for structural safety, the samples for extreme wind speeds for certain return periods at mountainous areas can only come from field measurements at construction site. However, wind speeds measuring duration is usually short in real practice. This work proposes a novel method for calculating extreme wind speeds in mountainous areas by using short-term field measurement data and long-term nearby meteorological observatory data. Extreme wind speeds in mountainous area are affected by mixed climates composed by local-scale wind and large-scale synoptic wind. The local winds can be recorded at construction site with short observatory time, while the extreme wind speeds samples from synoptic wind climate from nearby meteorological station with long observatory time is extracted for data augmentation. The bridge construction site at Hengduan Mountains in southwestern China is taken as an example in this study. A 10-month dataset of field measurement wind speeds is recorded at this location. This study firstly provides a new method to extract wind speed time series of windstorms. Based on the different windstorm features, the local and synoptic winds are separated. Next, the synoptic wind speeds from nearby meteorological stations are converted and combined with local winds to derive the extreme wind speeds probability distribution function. The calculation results shows that the extreme wind speed in the short return period is controlled by the local wind system, and the long-period extreme wind speed is determined by the synoptic wind system in the mountain area. The descending slope of the synoptic wind speed exceeding probability exceeds the local wind by about 20%. If the influence of mixed climate is not considered, and the wind speed samples are not divided by category, the decline slope will be 7% lower.

Keywords Extreme wind speed · Mountain wind system · Mixture climate · Data augmentation

✉ Wei Cui
cuiwei@tongji.edu.cn

Teng Ma
tengma@tongji.edu.cn

Lin Zhao
zhaolin@tongji.edu.cn

Ding Yejun
dyj@tongji.edu.cn

Fang Genshen
2222tjfgs@tongji.edu.cn

Yaojun Ge
yaojunge@tongji.edu.cn

[1] State Key Lab of Disaster Reduction in Civil Engineering, Tongji University, 1239 Siping Road, Shanghai 200092, China

[2] Key Laboratory of Transport Industry of Wind Resistant Technology for Bridge Structures, Tongji University, Shanghai, China

Published online: 07 November 2022

1 Introduction

Accurately estimating the extreme wind speeds with different recurrence periods is the first step for structure wind-resistant design, especially for flexible structures, such as long-span bridge and super-tall building. For example, the long-span bridge must sustain the aerodynamic stability (Simiu and Yeo 2019) in strong winds, and the tall building should provide sufficient habitability through mitigating wind-induced vibration (Kwok et al. 2009; Cui and Caracoglia 2020). In engineering practice, the structure must be designed to ensure the structural resistance larger than the wind loads, which is determined by local wind climate and normally prescribed in design code (ASCE 2016).

For the past decades, there are three the most widely used extreme wind speeds estimation methods based on extreme theory including annual maxima extreme method (Gumbel 2004), the peak-over-threshold (Simiu and Heckert 1996), and the method of independent storm (Cook 1982; Harris 1999). A lot of researches have gradually improved the extreme wind speed prediction of extreme theory, which will be reviewed in details following. At present, these methods are widely used at various places to provide extreme wind speed prediction with historical meteorological records (Palutikof et al. 1999).

Ideally, the extreme wind speeds should be calculated for the location at construction site. However, normally there is almost no long-term weather observation data at the exact construction site. In engineering practice, the regional extreme wind speed is calculated by the nearest weather observation station or refereed coded value in structural design standards (ASCE 2016) to serve as extreme wind speeds for the constructed structure. The above approach implies an assumption: The wind environment will remain constantly on the large spatial scale. This assumption is almost satisfied in flatland and plateau, because the strong wind events occur on the above two plain areas are generally macro-scale or meso-scale, such as typhoons and monsoons.

However, this assumption in mountainous areas is no longer valid, because the deep valley area separated by high mounts, and the wind climate in one valley cannot represent others. From the viewpoint of meteorology, the mountain wind system basically includes local mountain wind systems and synoptic wind systems (Li et al. 2014; Wagner 1938). Local mountainous wind systems form over valley terrain (Zardi and Whiteman 2013). Synoptic wind systems are normally referred as macro-scale wind phenomena (Jackson et al. 2013). The mountain topography only affects a local region. In addition, existing researches of mountainous wind system including field measurement (Whiteman 1990; Mingjin et al. 2019; Zhang et al. 2020a), numerical simulation (Maurizi et al. 1998; Kim et al. 2000; Bitsuamlak et al. 2004; Cao et al. 2012) and wind tunnel test (Li et al. 2017, 2010) also proves that the speed of local wind systems vary from place to place, depending on many factors including terrain characteristics, ground cover, soil moisture, altitude and etc. Therefore, in mountainous areas, it is not accurate to use the extreme wind speed from the nearby weather station on the proposed structure in the other valley.

On the other hand, the large scale synoptic wind system simultaneously affect the whole mountain area. In order to establish the relationship between weather station and construction site, several approaches has been developed, including wind tunnel methods (Li et al. 2010), numerical simulation (Bitsuamlak et al. 2004; Kim et al. 2000) and long-term synchronized field measurement (Huang et al. 2019; Beine et al. 2001). However, to calculate the extreme wind speed at a specific construction site in mountainous area, the local wind system information must be considered, but above mentioned methods cannot provide sufficiently accurate extreme wind speed estimation. Boundary layer wind tunnel test is unable to reproduce a thermally driven wind system (Zhang et al. 2020b; Tse et al. 2020). Numerical simulation, which consumes a lot of computing power, is impractical to perform many times to generate sufficient large sample required by extreme value analysis (Abd-Elaal et al. 2018; Ren et al. 2018). Field measurement is a feasible solution (Jing et al. 2020), but sufficient long-term synchronized observation between proposed structure site and weather station will delay the construction schedule, which is economically unacceptable. Therefore, it is necessary to develop economical and feasible method to estimate the extreme method based on synchronized short-term ($\leq$ 1 year) in mountainous area.

To improve the accuracy of statistical predictions based on short time wind observation, several researches use the information provided by another highly correlated data with a much longer observation time (Wang 2001; Gaidai et al. 2019). Due to the special features of the mountain wind system, the records of different observatories are only highly correlated for synoptic wind systems. The local mountain wind systems are normally confined in associate small region enclosed by nearby terrain formation, thus, the records of local mountain wind from different places are irrelevant.

In summery, the extreme wind events in mountainous areas should be considered as mixture climate including large scale synoptic winds and micro-scale local mountain wind systems (Gomes and Vickery 1978; Cook et al. 2003;

Cook 2004). In order to identify different wind systems from unlabeled wind speed data, several methods have been proposed including feature-based (De Gaetano et al. 2014), history-based (Lombardo et al. 2009) and data-based (Cui et al. 2021; Chen and Lombardo 2020). However, those methods are seldom applied in mountainous area. In this study, feature-based method is used to classify local mountain wind systems and synoptic wind systems. For the wind observation records, a short-term field measurement from self-installed equipment has been acquired to provide the information of local mountain wind systems and long-term observation data from nearby public weather station is employed to provide synoptic wind systems data.

An improved method of wind storms identification in mountainous areas is proposed in this paper, which can applied for both short-term measurement with high recording frequency and long-term measurement with low recording frequency. Then, different extreme value distribution models are employed to fit the identified two wind systems. Finally, the extreme wind speed is calculated for different recurrence periods by extreme value theory with mixture wind climate. A flow chart of research work is shown in Fig. 1.

2 Theoretical background

For structural design, safety considerations must be balanced against the additional cost of over design. Accurate estimation of the occurrence of extreme wind speeds is an important factor in achieving the correct balance. Typically, for most users of wind data, estimates of the 50-year return period extreme wind speed are required, based on 10 20 (and often fewer) available years of observations. For this situation, the data are generally fitted to a theoretical distribution in order to calculate the quartiles. In this section, several extreme wind speed statistic theory are described, including annual extreme method, method of independent storm and upcrossing method.

2.1 Gumbel with annual extremes

Fisher and Tippett (1928) showed that if a sample of n cases is chosen from a parent distribution, and the maximum of each sample is selected, then the distribution of the maximum approaches one of three limiting forms as the size of the samples increases. Gumbel (2004) argued that, in the case of floods, each year of record constitutes a sample with 365 cases and that the annual extreme flood is the maximum value of the sample. Thus, the Fisher Tippett distributions could be fitted to the set of annual maxima. This is the basis of all classical extreme value theory. The aim is to define the form of the limiting distribution and estimate the parameters, so that quartile value X_T can be calculated.

Fish-Tippett Type I distribution (also known as Gumbel distribution) has the cumulative distribution function:

$$P(u \le U) = \exp\left[-\left(\exp\left(-\frac{U-\beta}{\alpha}\right)\right)\right] \tag{1}$$

where β is the location parameter and α is the scale parameter.

Gumbel distribution is most widely used in wind-resistance code around world (ASCE 2016). Equation (1) calculates the probability that the wind speed does not exceed U in one year. Extreme wind speed of a certain return period R means annual exceed probability of this wind speed equals to $\frac{1}{R+1}$.

The great advantage of using the GEV distribution [Eq. (2)] with annual maximum is that few decisions are required during the calculation of the distribution parameters and quartiles. However, it requires a sufficient long wind observation time to provide enough extreme value samples.

$$P(u \le U) = \exp\left[-\left(1 - c\frac{U-\beta}{\alpha}\right)^{\frac{1}{c}}\right] \tag{2}$$

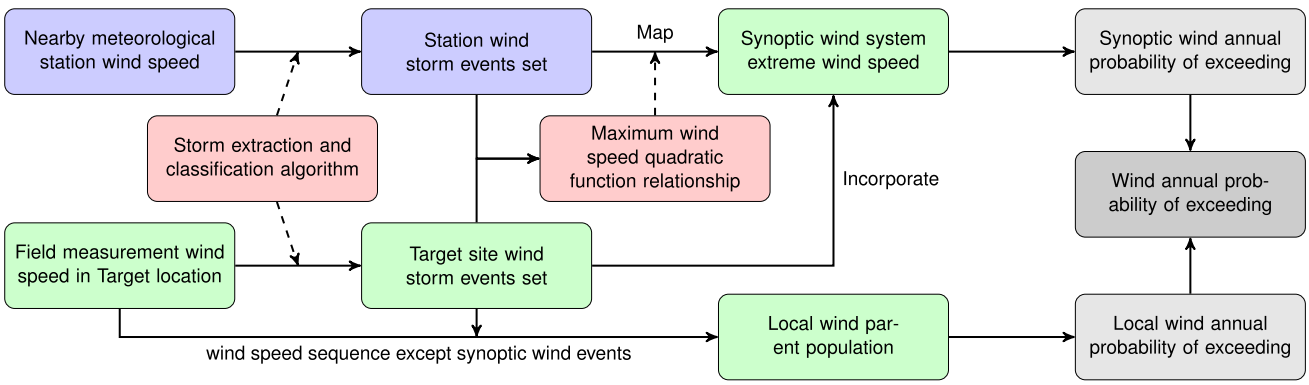

Fig. 1 Flow chart of extreme wind speed prediction in mountainous area

where β is the location parameter, α is the scale parameter and c is the shape parameter.

2.2 Method of independent storm

The principal drawback to the classical Gumbel method is that only one value is selected per epoch (e.g. one year). This greatly reduces the extreme data samples available for analysis, such that the underlying datasets must be long. This method is not suggested to be employed with fewer than 10 years. To increase the number of cases for analysis, method of independent storms (MIS) had been developed (Cook 1982; Harris 1999).

MIS increases the number of extreme available for analysis, whilst ensuring their independence by separating the parent time series of wind speeds into independent storms and then selecting the highest value from each storm. The storms is separated by a lull (period of wind speeds below a selected low threshold). Cook (1982) found a typical storm frequency rate to be around 100 events/year. After pre-processing, the extreme wind speed sample is fitted to the Gumbel distribution. Harris (1999) introduced two improvements to the MIS. This method modified the plotting position used by Cook (1982) to avoid systematic errors and fitted the distribution is given. The extreme wind speed exceed probability could be calculated by Poisson process [Eq. (3)]

$$P_T(u \le U) = \sum_{i=0}^{\infty} \frac{P(u \le U)^i [rT]^i \exp(-rT)}{i!} = \exp\{-rT[(1 - P(u \le U))]\} \tag{3}$$

where i is the number of occurrences, r is the rate of independent events per unit time, T is the epoch and $P(u \le U)$ is the Cumulative Distribution Function of gumbel distribution fitted by independent storms wind speed sample. When T equals to 1, Eq. (3) is used to calculated annual extreme wind speed exceed probability.

2.3 Upcrossing method

When the available wind speed data is further reduced, only a few years or less, the data utilization of MIS is also not enough. In this case, Gomes and Vickery (1977) suggested a method to estimate extreme wind speeds from the parameters of the parent distribution. This method is based on continue wind speed data from the site of interest. The average number of upcrossings of u per unit time (crossings with positive slope) can be obtained using Rice's formula (Rice 1944).

$$U^+(u) = \int_0^{\infty} \dot{u} f_{u,\dot{u}}(u, \dot{u}) d\dot{u} \tag{4}$$

in which $U^+(u)$ is the crossing rate and $f_{u,\dot{u}}(u, \dot{u})$ is the joint probability distribution of the mean wind speed and the rate of change of the wind speed. Assuming that u and $\dot{u}$ are independent and uncorrelated, and further assuming that $\dot{u}$ is a stationary Gaussian process with zero mean, Eq. (4) could be rewritten as:

$$U^+(u) = \frac{\sigma_{\dot{u}}}{\sqrt{2\pi}} f_v(v) \tag{5}$$

Equation (5) yields an expression for the excepted number of crossing per unit time for a threshold. Assuming these crossings to be rare and independent events, the probability of exceed can be modeled using a Poisson approximation:

$$P_T(u \le U) = 1 - e^{U^+(u)T} \tag{6}$$

2.4 Mixed climate theory

The technique for mixed wind climate extreme wind speed calculation required a separate extreme-value analysis of the values stemming from each significant wind-producing mechanism, followed by synthesis of the individual mechanisms into a composite extreme-value distribution. Gomes and Vickery (1978) carried out the different causative mechanisms extreme wind speed analysis for Australia and America.

Consider two wind independent mechanisms A and B, giving sets of wind speeds U_A and U_B, respectively, from each. The cumulative probability $P_T(u < U)$ of the maximum value u from either mechanism in an epoch T is less than some value U could be calculated by

$$P_T(u < U) = P_T(u_B < U) \times P_T(u_A < U) \tag{7}$$

where u_A, u_B is the wind speed from mechanism A or B.

Equation (7) could only be used if T is long enough that each mechanism events are sufficiently frequent to occur in every epoch.

3 The measurement equipment and recorded data

The construction site of Murong Bridge in China is employed as the research object. This section describes the topography and location of Murong Bridge, the installation of the wind recording system and the general description of wind speed data from field measurement and weather observation station.

3.1 Description of the bridge site

The study area of this work is in southwestern China, which is located on the Xianshui River in Yajiang County, Ganzi Prefecture, Sichuan Province specifically. It is in the middle of the Hengduan Mountain Range, which is in the southeastern of the Tibetan Plateau. Figure 2 shows the location of the study area in the view of macro-scale.

The bridge site located at the Hengduan Mountains of southwestern China is a typical narrowed V-shaped deep-cut canyon and the depth of the canyon is about 500-1500 meters. Altitude around the bridge site is 3900-4800 meters. Moreover, the lower reaches of the river are meandering and topography near the bridge varies dramatically. The terrain at the bridge site is shown as Fig. 3.

3.2 Installation of the wind measuring system on Murong bridge

The site observation station had been placed on the top of the construction tower crane. It was 20 meters higher than the main beam, so wind speed accuracy is less affected by the structure. As shown in Fig. 4, the wind measuring system includes one 3 Axis Ultrasonic anemometer (WindMaster, 32Hz sampling rate, measurement range 0-50 m/s) and one propeller anemometer (RM Young 05103, measurement range 0-60 m/s). The propeller anemometers is a mechanical anemometer composed by a propeller to collect wind speed data. The ultrasonic anemometer measures 3D wind speed based on the transit time of ultrasonic acoustic signals. The data recorded contain instantaneous wind speed in longitudinal (North-South direction), lateral (East-West direction) and vertical directions.The short-term monitored wind data, which were collected from this system, used for this study covered a 10 month period from December 2019 to September 2020.

3.3 Observation of meteorological station

Besides the on-site short-term wind speeds measurement, long-term regional wind speed data with large sample of synoptic strong wind events is also needed for extreme wind speed calculation in mountainous area. The nearest meteorological observatory is DAWU station, which is located in the same canyon (Xianshui River Canyon) with Murong Bridge. The spatial relationship between Murong Bridge and DAWU station and region terrine are shown in Fig. 5. The direct distance between Murong and DAWU is about 70 km.

When one synoptic wind system approaches this area, both Murong and DAWU will be affected simultaneously with short temporal delay. So the wind speed record from DAWU can be used to predict the extreme speeds from synoptic winds in Murong. Data source of DAWU station is downloaded from Global Integrated Surface Dataset

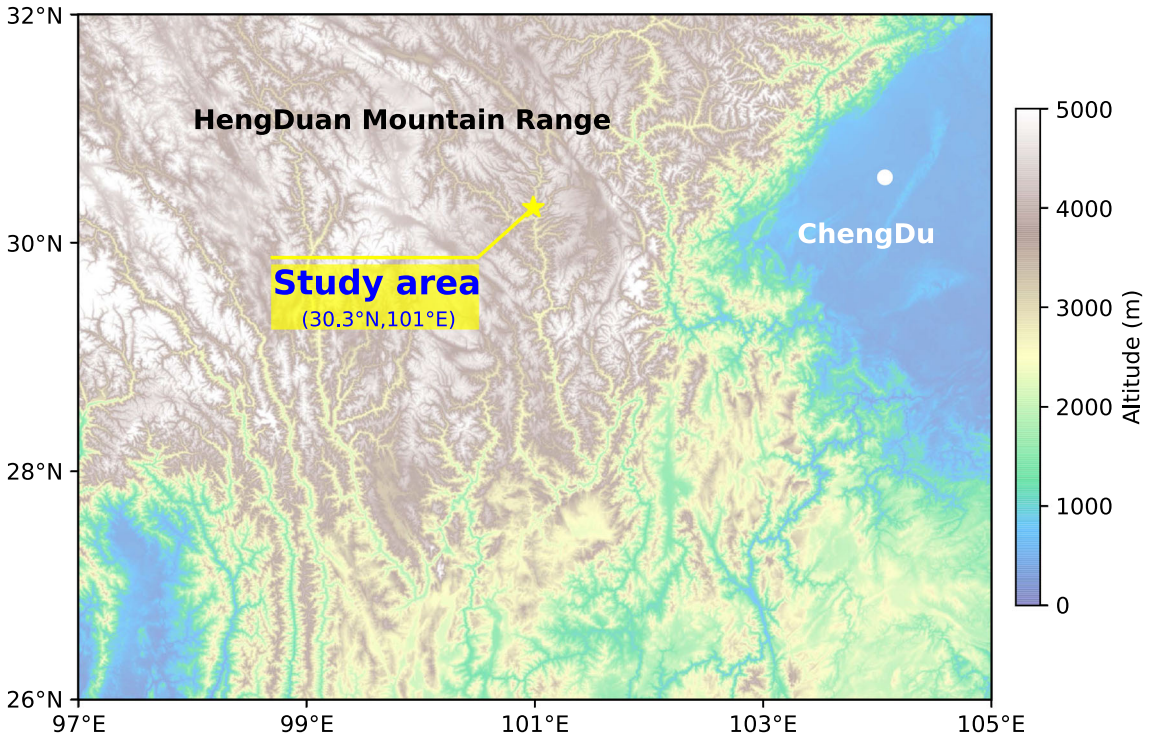

Fig. 2 The location of study area

Fig. 3 Terrain at the bridge site (Captured from Google Earth, 25 km around the bridge site)

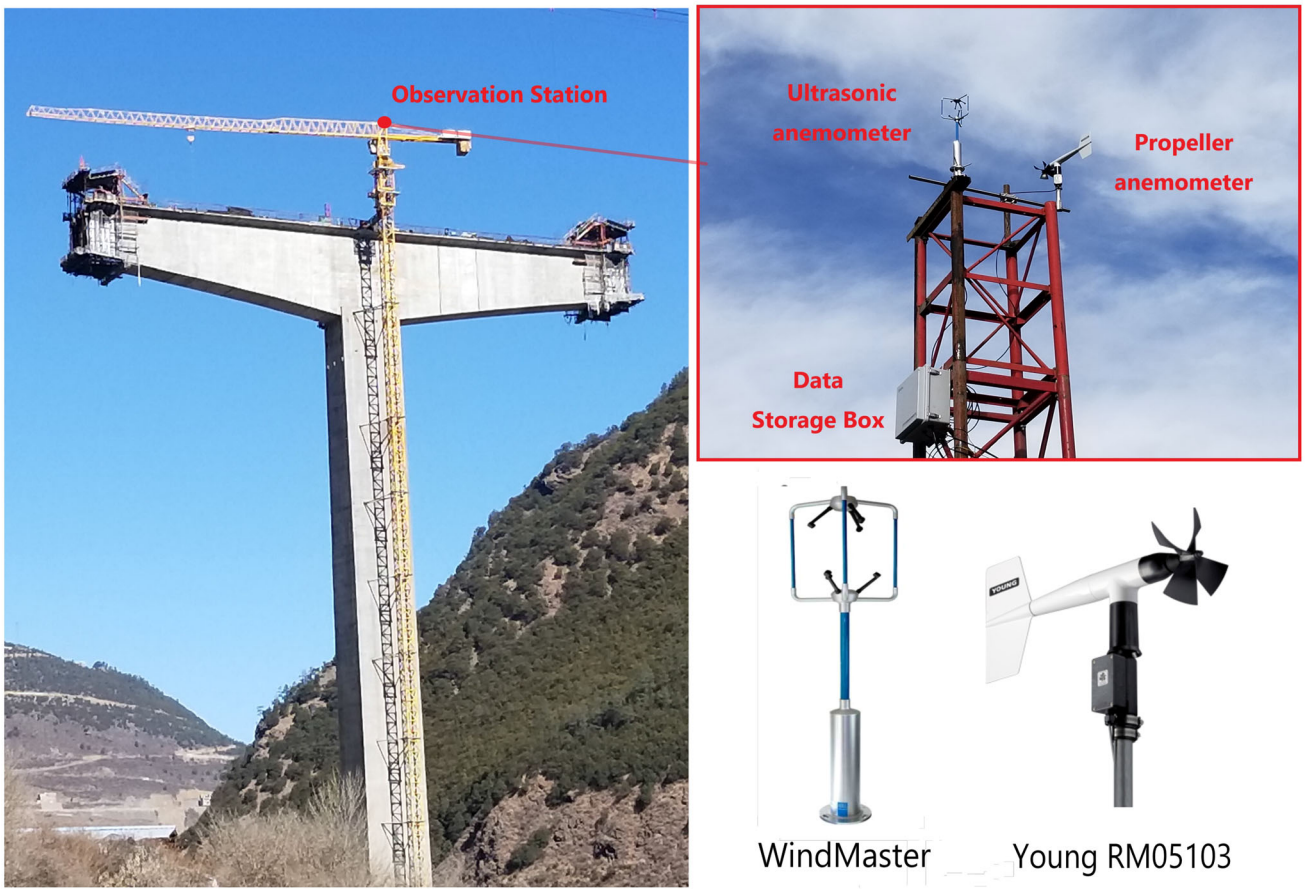

Fig. 4 The onsite meteorological observation station location (left), the close-up view of anemometers (upper right) and the anemometers

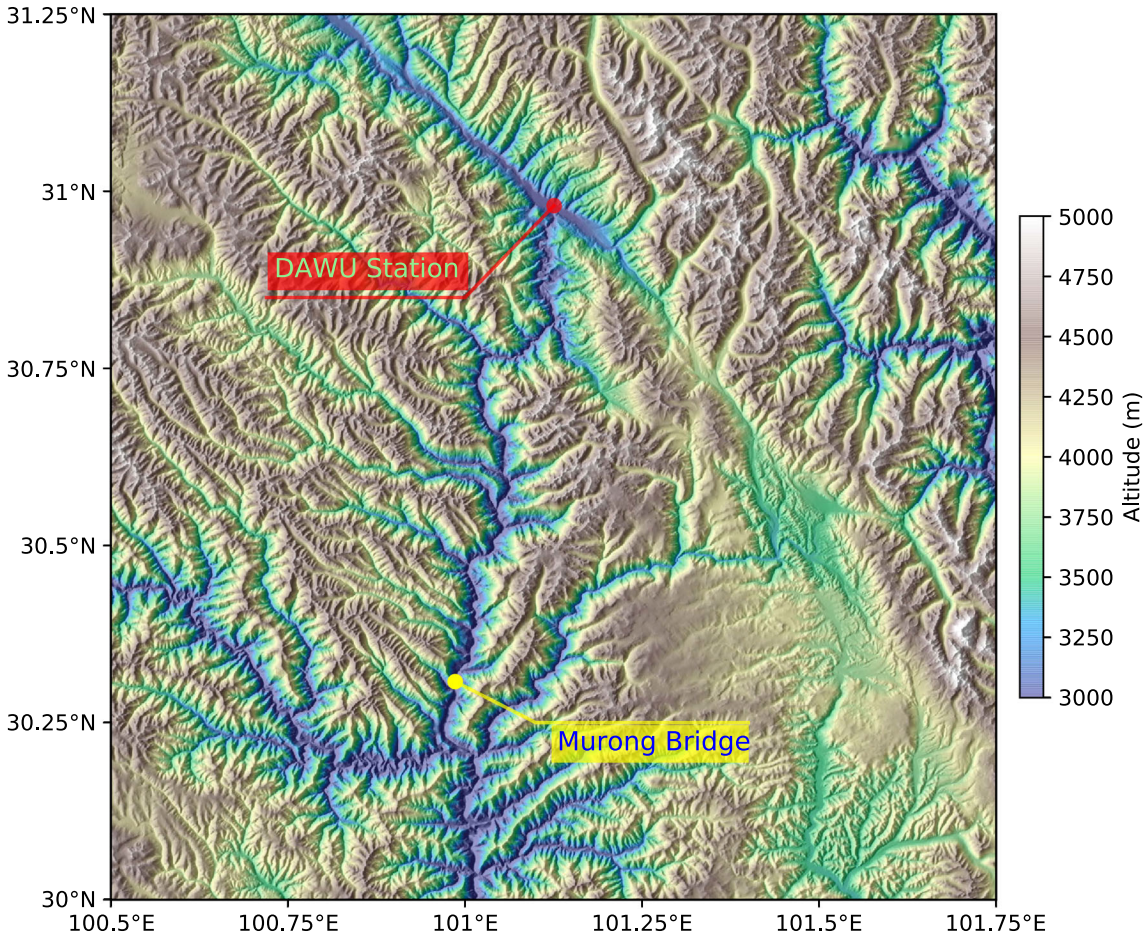

Fig. 5 Location relationship between DAWU station and Murong and surrounding terrain

from National Climatic Data Center (NCDC) (Young et al. 2018) (https://www.ncei.noaa.gov/access/search/data-search/global-hourly). The station ID is 561670. It has recorded meteorological data since 1979-07-01. Data type covers wind-observation, hourly liquid-precipitation, sky condition, air temperature, sea level pressure. Total 30 years wind-observation history from 1990 to 2020 are used in this study since data before 1990 was recorded manually with less credibility.

4 Wind system extraction and classification

In order to calculate the extreme wind speed in mountainous area, it is necessary to classify and then extract the local wind events and synoptic wind events from original continuous wind speed records. The strong wind events extraction algorithm based on feature points is described firstly in this section. Wind event characteristics of different wind systems are analyzed later. Based on these characteristics, the wind event type classification method is proposed.

4.1 Wind events identification and extraction algorithm

There are two purposes of wind events extraction. One is creating the basic data set of wind speed extremes. The other is classifying different wind event types from original wind speed data. The wind events extraction algorithm needs to find each event sequence with the maximum wind speed above a predefined threshold from a long continuous wind speed data. Each wind event sequence must contain the whole process of wind event from the beginning to the

end, in order to identify the type of each wind event. This is different from the method of independent storm, which only ensure the independence between storms but not require the whole process of storm. The whole process of wind events contains necessary information for category recognition. So a new storm extraction algorithm based on feature points is proposed.

The feature point is the demarcation point in the time series where can the changes of sequence trending occurs (Deng et al. 2013; Pavan et al. 2017). It is aimed to find all peaks and valleys, termed as landmarks, from time series (Zhao and Itti 2015). It has been applied widely in the research field of the trend of the time series (Fulcher and Jones 2014; Simo-Serra et al. 2015). In a discrete wind speed time series sequence $U(t) = (U_1, U_2, ..., U_n)$, all the wind speed points i that meet $(U_i - U_{i-1})(U_{i+1} - U_i) < 0$ are reorganized into a new sequence $U' = (U'_1, U'_2, ..., U'_m)$. U' is the maximum point set of original wind speed $U(t)$. In new sequence U', each points that meet $(U'_i - U'_{i-1} - \varepsilon)(U'_i - U'_{i+1}) > 0$ or $(U'_i - U'_{i+1} - \varepsilon)(U'_i - U'_{i-1}) > 0$ are feature points (ε is a positive hyper-parameter). Feature points set is second-order difference maximum point of original sequence. The purpose of second-order difference is to avoid local non-trend maximum point interference wind event extraction algorithm.

Extraction feature points process could be described as Algorithm 1.

Here's example to explain feature points algorithm specifically by Fig. 6. Original wind speed extracted from DAWU meteorological station represents $U(t)$. As Fig. 6 shown, $U'(t)$ (red star) is a set that satisfies $u_i > u_{i-1}$ and $u_i > u_{i+1}$. In the view of mathematical, $U'(t)$ is the first-order derivative changing points set of $U(t)$. The feature points of continued records U(t) are the peaks of wind speeds, which are the highest points of each wind events. ε is used to avoid small fluctuations being misidentified as wind events feature points. Without ϵ, some small variety will be identified wrongly as feature points like green dashed circle in Fig. 6.

In the wind speed time series, each strong wind event starts with a low wind speed, and then develops to high wind speed, and finally reaches to the end with low wind speed. The above algorithm could find the wind speed peak index of each wind event, regardless of the sampling rate of the wind speed sequence. The start point and the end point of event could be iteratively searched out on both sides of feature points. The condition for stopping iterative search is wind speed is lower than the static wind speed V_s for a period of time Δt.

Hyper-parameters determination decides the performance of algorithm and accuracy of extreme wind speed prediction. There are three hyper-parameters need to be chosen. The algorithm ignores feature points whose fluctuation range is less than the parameter ε. Considering the

Algorithm 1 Wind event feature point detection

Require: $U_t = (u_{t1}, u_{t2}, ..., u_{tn})$, ε:float
1: $FPs \Leftarrow [\,]$
2: $U'_t \Leftarrow \text{diff}(U_t)$
3: index $\Leftarrow$ find(U'_t(1:end-1)*U'_t(2:end)<0)+1)
4: **for** i $\leftarrow$ 2:(size($index$)-1) **do**
5: $Judge^l_1 = U_t(index(\text{i})) > U_t(index(\text{i-1}) + \varepsilon$
6: $Judge^n_1 = U_t(index(\text{i})) > U_t(index(\text{i+1})$
7: $Judge^l_2 = U_t(index(\text{i})) > U_t(index(\text{i+1}) + \varepsilon$
8: $Judge^n_2 = U_t(index(\text{i})) > U_t(index(\text{i-1})$
9: **end for**
10: **if** ($Judge^l_1$ and $Judge^n_1$) or ($Judge^l_2$ and $Judge^n_2$) **then**
11: $FPs \leftarrow \text{add}(index(\text{i}))$
12: **end if**
13: **return** FPs:FeaturePoints

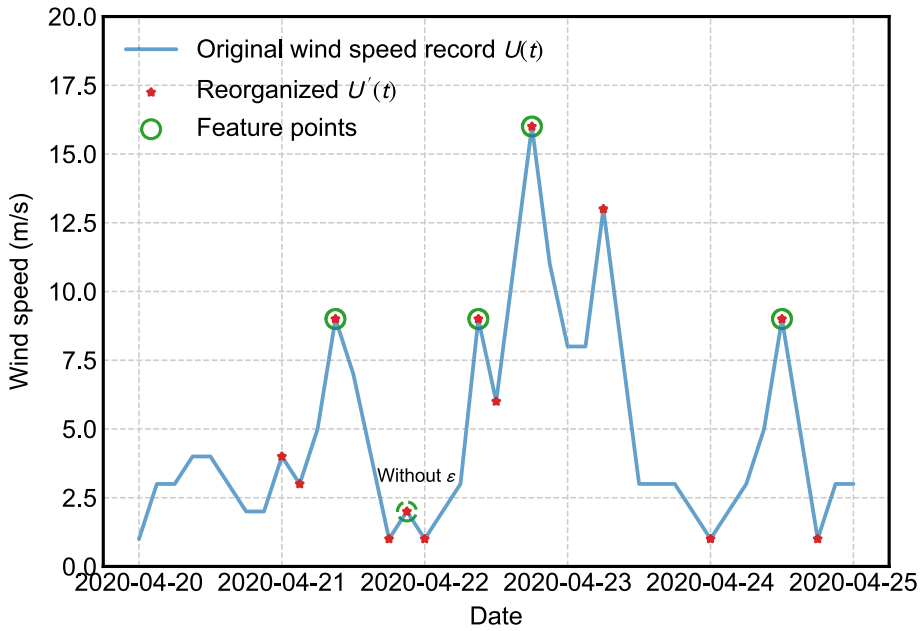

Fig. 6 The example of wind event feature point detection algorithm

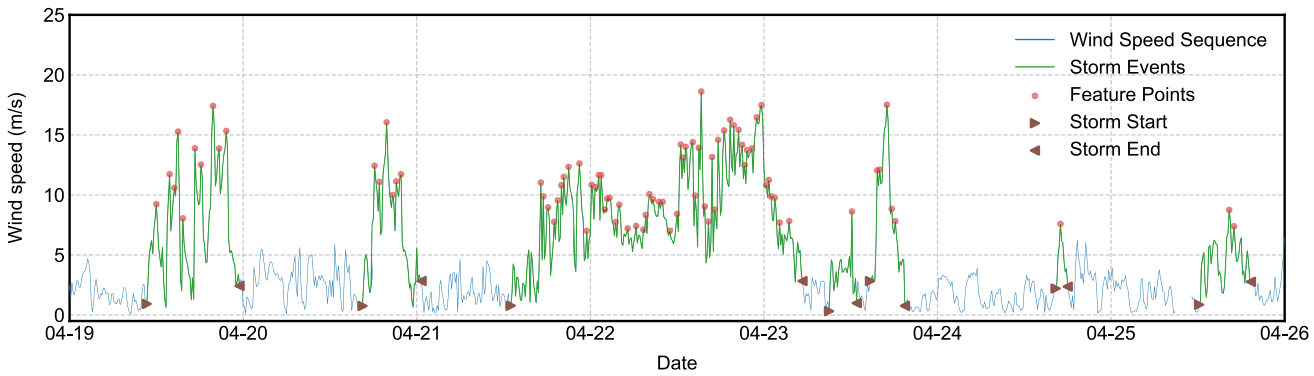

Fig. 7 Wind event extraction algorithm processing high-frequency wind speed sequence (Data source: Murong Bridge field measurement; Sampling period: 10 min)

characteristics of wind speed sequence in Murong area, these hyper-parameters are chosen manually: $\varepsilon = 1$ m/s; $V_s = 2$ m/s; $\Delta t = 1$ hour. That means a wind event is terminated when wind speed consistently below 2m/s for more than an hour. These hyper-parameters may be only suitable for this case. It's difficult to propose a metric to optimize hyper-parameters.

In order to verify the effectiveness and robustness of the wind event extraction algorithm, Figs. 7 and 8 show the result of algorithm on datasets with different sampling rate. The wind event extraction algorithm based on feature points and iterative search has good effects on wind speed sequences of different sampling rates.

4.2 Characteristics of two typical mountainous Wind events

According to features of mountainous wind system, strong wind events are divided into local mountain wind systems and synoptic wind systems. In order to classify, this section will analyze the characteristics of these two wind systems.

A power-spectrum analysis of wind speed in Murong is plotted in Fig. 9. There appear to be two major energy peaks in the spectrum; blue peak (local wind system) occurs at a period of about 24 hours, and red peak (synoptic wind system) occurs at a period of 7-15 days, which is similar as van der Hoven's spectrum (van der Hoven

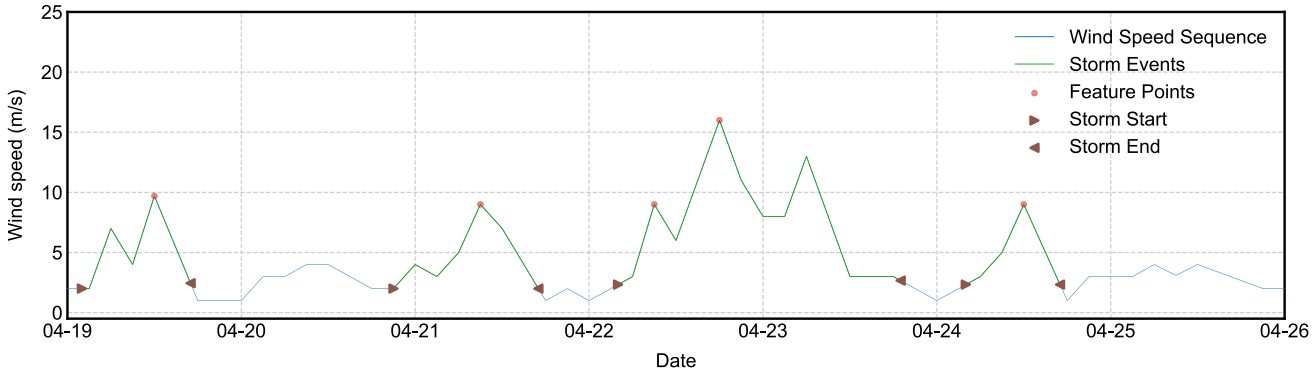

Fig. 8 Wind event extraction algorithm processing low-frequency wind speed sequence (Data source: DAWU Station; Sampling period: 3 h)

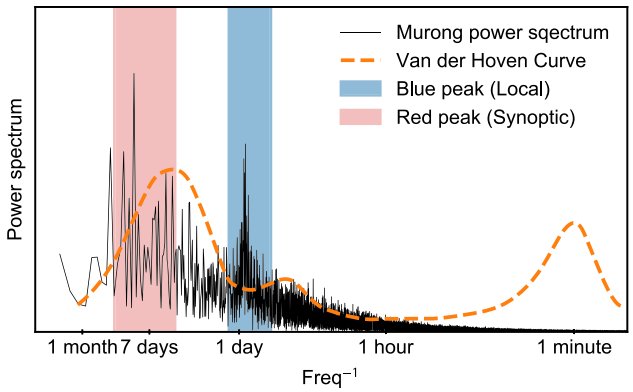

Fig. 9 Power spectrum of Murong wind speed and comparison with van Der Hoven's curve

1957). The reason of the different peaks is that the mountainous wind systems is a different meteorological process with plain terrain. Mountainous terrain generates local temperature gradients everyday, leading to local wind system. In non-mountainous cities, the modified van der Hoven spectrum also has a one-day peak, but the cause of this peak is the urban heat island effect.

Based on the definition of mountainous wind system and the analysis of the field measured data, the characteristics of the mountainous wind system are summarized following. Local mountainous wind system occurs everyday. Since it is driven by diurnal variation of local temperature, the duration of local mountainous wind system are normally much shorter than synoptic wind events. In addition, because of complex terrain in mountainous area shown in Fig. 5, the local wind system at different locations are almost irrelevant. In contrast, the "power" driving synoptic wind system is much stronger than local mountainous wind system. So it will affect large region with longer duration and higher wind speed rather than being confined in a specific area. When synoptic wind system occur, the wind event could be recorded by all station nearby concurrently.

4.3 Storm type classification method

The most important differences between local mountain wind and synoptic wind are the occurring frequency and duration of the wind storm. Frequency is how often a certain type wind event occurs. The frequency information is not available before wind event identification. So, the other characteristics are used to establish a wind event type classification algorithm. For each wind speed sub-sequence extracted by wind event identification algorithm, sequence length which represents duration could be used as a classification metric. In addition, the wind speed metric needs to indicate the proportion of low wind speeds in sub-sequence. Wind direction is a key feature for wind storm classification in general, especially in the difference between typhoon and non-typhoon (Cui et al. 2021). However, mountainous deep canyon is a specific case for wind system. Local and synoptic wind systems are restricted in a specific direction by canyon topography. The wind speed frequency diagram of Murong are shown in Fig. 11, which has only two main directions at 22.5 and 210. The main wind directions are same as the trend of canyon, whatever the type of wind storm is. So the wind direction could not be used to identify local and synoptic wind.

Wind event duration and low-speed ratio are used to identify synoptic wind and local wind events. Wind event duration means how long a wind event lasts. The low-speed ratio is the ratio of low wind speed data points to the total. An assumption is applied that all mountain wind events include only two types: synoptic wind and local wind. Therefore, synoptic wind events are only defined and remaining wind events are local. Normally, synoptic wind events have greater energy source and a wider range of influence. It can be inferred that synoptic winds last longer. So synoptic wind storms should satisfy two judgments at the same time. Firstly, its duration should be longer than 24

hours. And the second judgment is that low-speed ratio accounts for less than 50%. In Murong area, synoptic wind system is defined as a wind event with more than 24 hours duration and low-speed time (wind speed is lower than 4 m/s) accounts for less than 50%. Figure 12 shows how these two judgments works in real wind speed data from Murong meteorological station.

The classification method is verified though the comparison between field measurement data at Murong and meteorological data at DAWU. The verified metric is the time overlap ratio between synoptic wind system in Murong and DAWU. As shown in Fig. 10, time overlap is the time period during when two wind events recorded by different observatory are overlapped. Because one synoptic wind system will affect Murong site and DAWU meteorological observatory simultaneously during in a certain period. From December 2019 to September 2020, 184 wind event sub-sequences are extracted from original sequence recorded by Murong construction site, including 6 synoptic wind system. In DAWU station, wind event extraction algorithm finds 1334 wind event since 1990. The maximum wind speed and duration distribution of wind events are shown in Figs. 13 and 14. Maximum wind speed is the maximum value of a wind event wind speed records. The distribution of duration shows that long-duration wind events account for a small part of all wind event, which conforms to the definition and frequency feature of synoptic wind events. According to classification metrics, synoptic wind events information and visualization from two stations recorded from December 2019 to September 2020 is shown in Table 1 and Fig. 16. The records of each synoptic wind event at different stations have a high time overlap ratio.

Field measurement always could not last for a long time, especially in real construction practice. Wind speed at Murong in October and November are not recorded in this work because of some objective reasons in construction. Wind speed measurement for less than one year might influence the results of extreme wind speed analysis. And this influence must be discussed. Local and synoptic wind system occurring frequency from 30 years DAWU meteorological station records are shown in Fig. 15. It could be clearly seen that winter wind system is infrequent compared with other seasons.

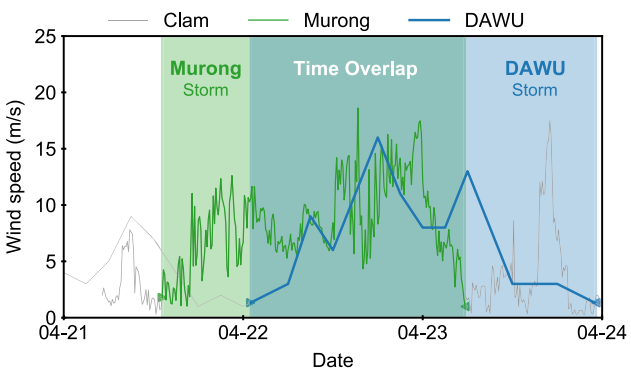

Fig. 10 An example of time overlap

5 Mixture climate extreme wind speed calculation

Mountainous wind system is a mixture climate system composed of local mountainous wind system and synoptic wind system. These two wind system should be analyzed separately for extreme wind speed calculation. Rely on the wind speed records from Murong field measurement and DAWU observatory, two calculation case studies are carried out to discuss the extreme wind speed in mixture mountainous wind system. The primary case focus on DAWU station, which has long-term wind speed records. The advanced case is for Murong Bridge, which is a real construction site with short-term field measurement records.

5.1 First case: calculation extreme wind speed for DAWU meteorological station

We begin by considering the mountainous extreme wind speed problem of meteorological station. In this case, the wind speed record is long enough to calculate different

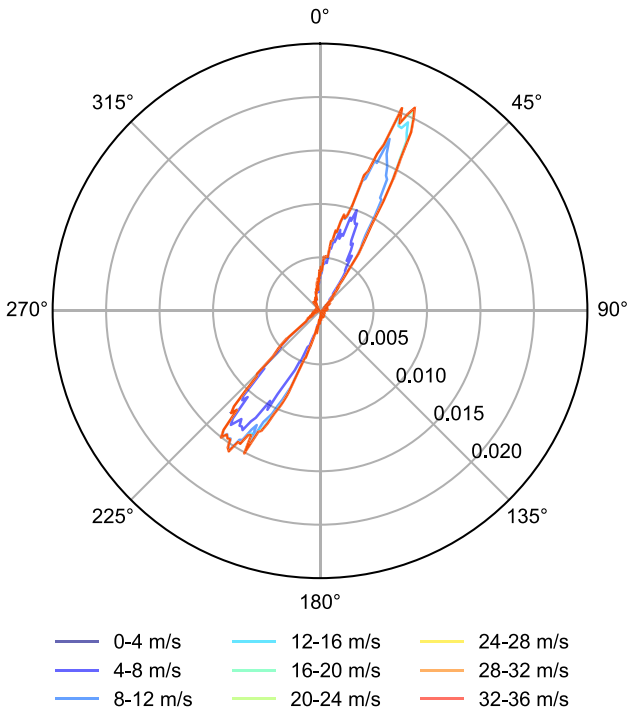

Fig. 11 The wind speed frequency diagram of Murong

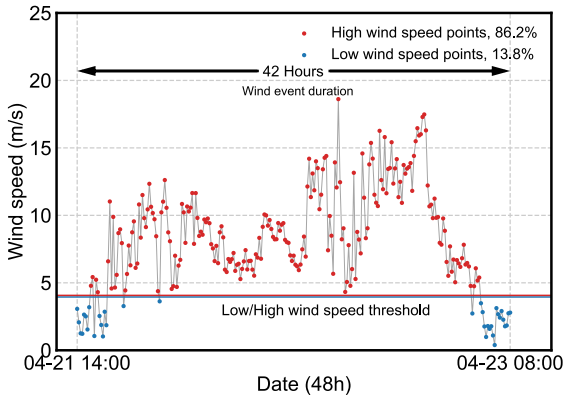

(a) Synoptic wind event sample

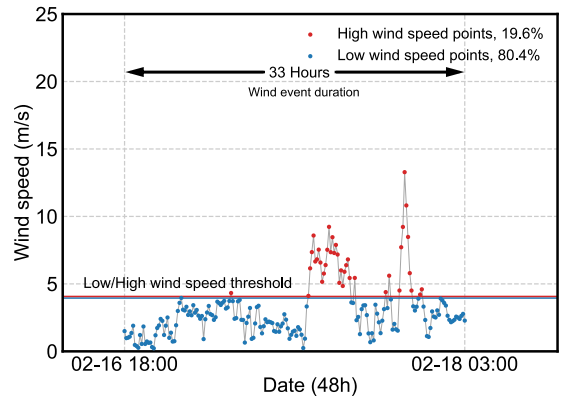

(b) Local wind event sample(low-speed ratio judgement)

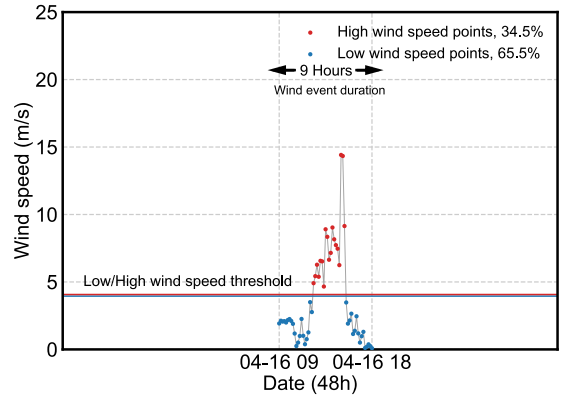

(c) Local wind event sample(wind event duration judgement)

Fig. 12 Example of wind event classification judgment criteria: wind event duration and low-speed ratio

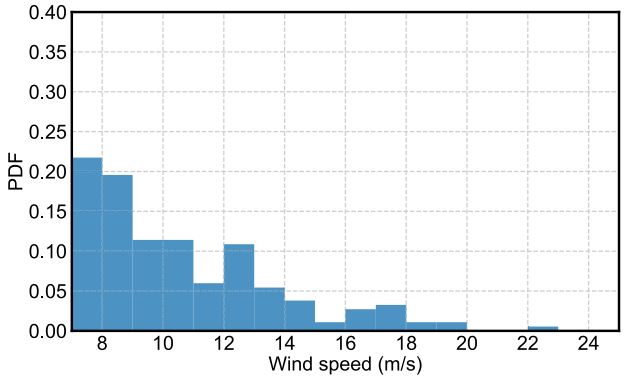

(a) Maximum wind speed

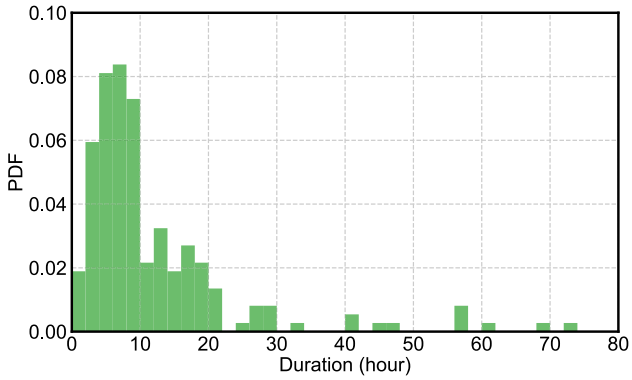

(b) Duration

Fig. 13 Histogram of wind event features extracted from Murong observatory from December 2019 to September 2020 (184 wind events)

wind system including synoptic and local. So this case will only focus on the characteristics of mixture wind climate in mountainous areas and discuss whether this method is useful for mountainous area.

DAWU is an example for this case, which has more than 30 years of wind speed records. The records from 1990 to 2020 is used to calculate the extreme wind speed. Totally, 1334 wind events are extracted by 30-year wind speeds records by using wind events identification and extraction algorithm in Sect. 4. These wind events can be divided into 202 synoptic wind events and 1132 local wind events by two judgments including wind event duration and low-speed ratio. The maximum wind speed value of each wind event is extracted to form an extreme value sample of "Method of independent storm".

All distribution parameters estimation is calculated in the python program by using scipy.stats library. In order to fit the tail of distribution well, the maximum likelihood method is used in this work. The distribution parameters estimated by the maximum likelihood method are shown in Table 2. Local and synoptic extreme wind speed samples are used to fit the Gumbel [Eq. (1)] distribution. And Akaike information criterion (AIC) and Bayesian information criterion (BIC) are used to quantitative fitting performance. AIC and BIC metrics are calculated by Eq. (8)(9).

$$AIC = 2k - 2ln(likelihood) \tag{8}$$

$$BIC = kln(N) - 2ln(likelihood) \tag{9}$$

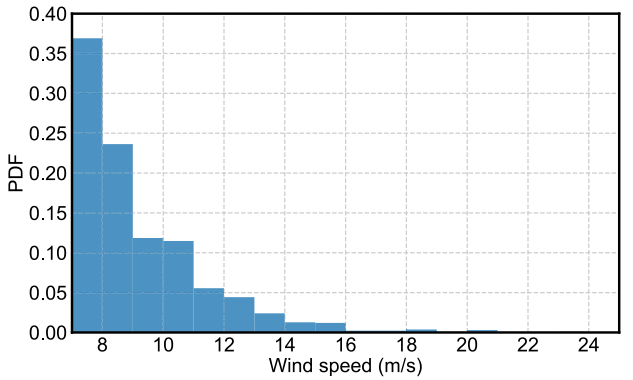

(a) Maximum wind speed

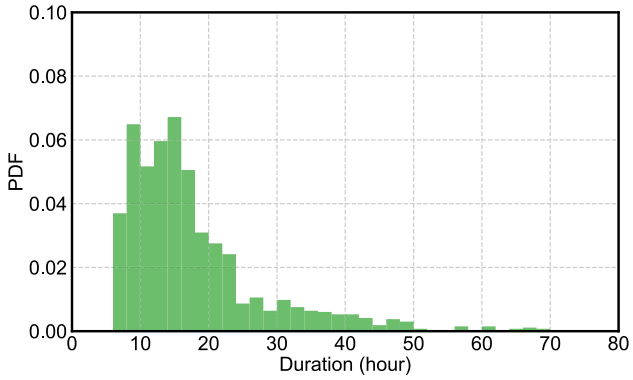

(b) Duration

Fig. 14 Histogram of wind event features extracted from DAWU station from January 1990 to September 2020 (1334 wind events)

where k is the parameter number of distribution, N is the number of observations. The likelihood is the sum of observations probability density function.

Figures 17, 18 and 19 are used to show which distribution is more suitable for different extreme wind samples. Figures 17 and 18 shows the histogram of extreme wind speed observations and Gumbel distribution fitting curve. Figure 19 is a quantile-quantile plot of two sample fitted by Gumbel and GEV distribution. The quantitative result from AIC/BIC and visualization from Q-Q plot and histogram-curve all prove that Gumbel has a good fitting performance in this case.

According to the fitted Gumbel distribution, extreme wind speed could be calculated by Quartile. Quartile is the inverse of Cumulative distribution function (CDF), which means the extreme wind speed with specific probability. The annual probability that the maximum wind speed u of the synoptic wind system exceeds U can be expressed by Eq. (3).

The mixed wind system consists of local mountainous wind system and synoptic wind system. These two wind system events are independent. So within a year, the maximum wind speed does not exceed U is equivalent t that the maximum wind speed of local mountainous wind system and synoptic wind system does not exceed U, as Eq. (7).

Figure 20 shows the extreme wind speed calculation results by the above method. The slope of local(blue dash line) wind speed is lower than synoptic(red dotted-dash line), which is consistent with their shape parameters. That means the extreme wind speeds in different return periods are controlled by different types of wind events. Synoptic wind events play an important role in high return period. In this case, demarcation point is on around 300 years. The green solid line is mixed extreme wind speed curve, which is the envelope of local and synoptic. Comparing the mixed climate method and annual extreme method(thick black solid line), it can be seen that the annual extreme method is not applicable in calculating extreme wind speed in mountainous areas. This is because the annual extreme sample is mixed and could be divided into 76% Local wind and 24% Synoptic wind. Orange Points are from Chinese Code Wind-resistant Design Specification for Highway Bridges (Tongji-University 2018). The trend of Code is similar to mixed line, but the Chinese code are conservative with generalized extreme distribution fitting.

As Fig. 20 shown, the extreme wind speed curves increase almost linearly, and the slope is marked above each curve. The descending slope of the synoptic wind speed exceeding probability exceeds the local wind by about 20%. If the influence of mixed climate is not considered, and the wind speed samples are not divided by category, the decline slope will be 7% lower.

Table 1 Synoptic wind events information and overlap test

ID	1	2	3	4	5	6
Murong start	2/9 12:10	2/27 12:20	4/1 11:00	4/17 9:10	4/21 13:10	5/8 6:50
DAWU start	2/9 3:00	2/27 2:00	4/1 1:00	4/17 1:00	4/22 1:00	5/8 18:00
Murong end	2/10 4:30	2/28 9:40	4/3 23:50	4/18 11:40	4/23 5:40	5/9 4:40
DAWU end	2/10 0:00	2/28 2:00	4/2 20:00	4/17 21:00	4/23 23:00	5/9 17:00
Murong wind speed	16.3	11.9	14.7	12.9	18.6	17.2
DAWU wind speed	10.0	7.0	9.0	10.4	16.0	12.0
Overlap	70.83%	64.07%	54.25%	44.65%	70.78%	47.07%

5.2 Second case: calculation extreme wind speed for Murong bridge site

In previous case, extreme wind speed in a mountainous area with long-term wind speed records could be calculated. In this part, we will calculate the extreme wind speed of an actual mountainous construction site only with a short-term wind speed field measurement records. But this amount of field measurement data is much smaller than the requirement of extreme wind speed statistical model fitting.

For the local mountains wind system, it must be analyzed with field measurement data extracted from anemometer installed on the constructed bridge. Because of only 10 months recording time, the wind speed parent population is directly used based on uncrossing method (Gomes and Vickery 1977), which is based on Rice's formula (Rice 1944) for the uncrossing rate $U^+(u)$ of a stationary random function of time $U(t)$. On the other hand, for synoptic wind system, only 6 samples recorded within 10 month field measurement shown in Table 1 is insufficient to calculate the extreme wind speed of 50-year or longer return period. However, because of its large scale, very synoptic wind event will be recorded by the nearby meteorological observatory. If the synoptic wind event records of the meteorological observatory could be mapped to bridge construction site, there will be sufficient synoptic wind event data available.

The parent population of local wind event is all wind speed records in Murong except six synoptic wind events.

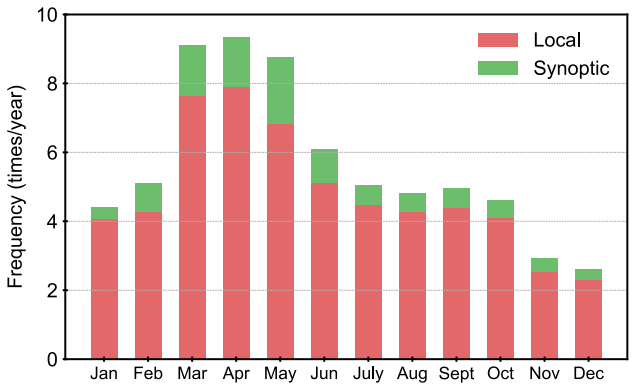

Fig. 15 Wind system occurring frequency from DAWU meteorological station records

Figure 22 illustrates the empirical histogram of the parent population of wind speed from December 2019 to September 2020 and corresponding PDF obtained from the Weibull model. Good correspondence between the raw data and the model confirms that the Weibull model is adequate to model the wind speed parent distribution. The cumulative distribution function could be written as Eq. (10).

$$P(u \le U) = 1 - \exp\left[\left(-\frac{x-\beta}{\alpha}\right)^c\right] \tag{10}$$

where β is the location parameter, α is the scale parameter and c is the shape parameter.

Through maximum likelihood method, the Weibull distribution parameter is estimated as Table 3 shown. And Fig. 21 shows the quantile-quantile plot of wind speed observation against distribution fitting result. The Weibull distribution with $\alpha = 3.229, \beta = 0.011, c = 1.189$ could stand for local wind event parent sample observations.

The correlation between wind speed U and the first derivative of wind speed $\dot{U}$ is -0.05, which proves that $U, \dot{U}$ are approximately independent. So Eq. (5) could be used to calculate $U^+(u)$. The annual exceed probability of local wind $P_D(u \le U)$ is calculated by Eq. (6) by $T = 1$.

Compared with local wind system, synoptic wind events is an less frequent phenomenon in mountainous wind climate. The extreme wind speed of synoptic wind events will be calculated by the method of Independent Storm too. The extreme value samples are divided into two parts, including Murong measurement data and DAWU data with wind speed mapping. Wind speed mapping is a converting formula of synoptic wind event from nearby meteorological observatory to the target site. In this study, each synoptic wind event are recorded at DAWU meteorological observatory and Murong field measurement. The topography and height of these two observations are different. In order to simplify the mapping process, this research only establishes the quadratic function relationship of the maximum wind speed in each wind event between DAWU station and Murong bridge deck.

The fitted line are shown in Fig. 23. By fitting the data in Table 1, Murong to DAWU converting function is a quadratic function with zero intercept. This fitting model shows that the maximum wind speed in synoptic wind

Table 2 Estimated parameter values and quantitative performance of different type wind event fitted by different distribution type

Wind event type	Estimated parameter values		Performance	
	Location	Scale	AIC	BIC
Local wind event	6.682	1.761	6902.565	6913.485
Synoptic wind event	7.397	2.056	1316.308	1323.682
Commingled wind event	6.774	1.823	8265.579	8276.813

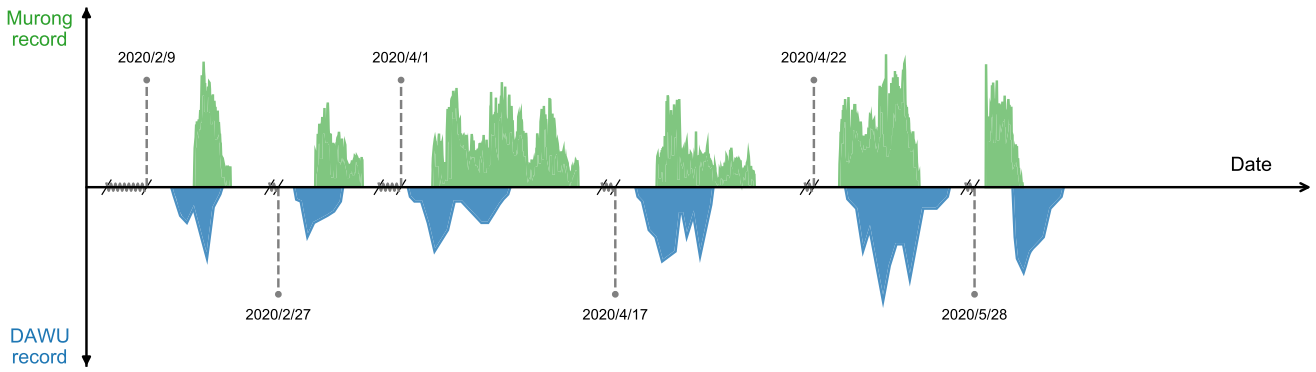

Fig. 16 Synoptic wind events information and overlap visualization

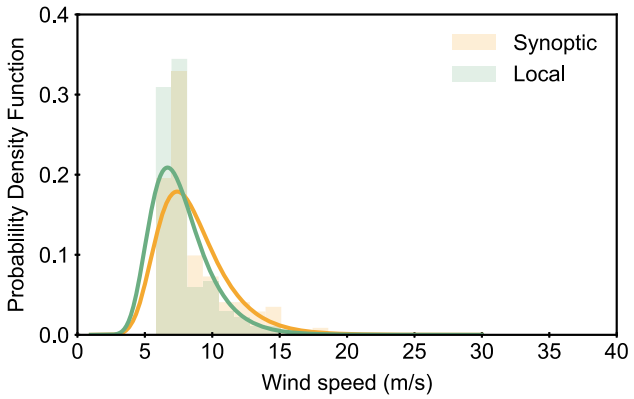

Fig. 17 Distribution of wind speed extreme sample from different system at DAWU, empirical histogram and PDF model (Gumbel)

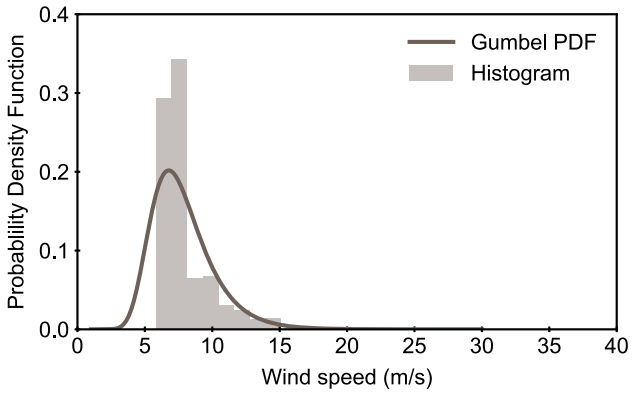

Fig. 18 Distribution of wind speed commingled extreme sample at DAWU, empirical histogram and PDF model (Gumbel)

event of two stations approximately starts from zero and increases at different rates. In addition, Murong station is about 200 meters height from the ground and DAWU is 10 meters. Therefore, the maximum wind speed recorded by Murong should be higher than DAWU under the influence of the same wind event.

After wind speed mapping, synoptic wind events extreme sample in Murong is ready to fit Gumbel

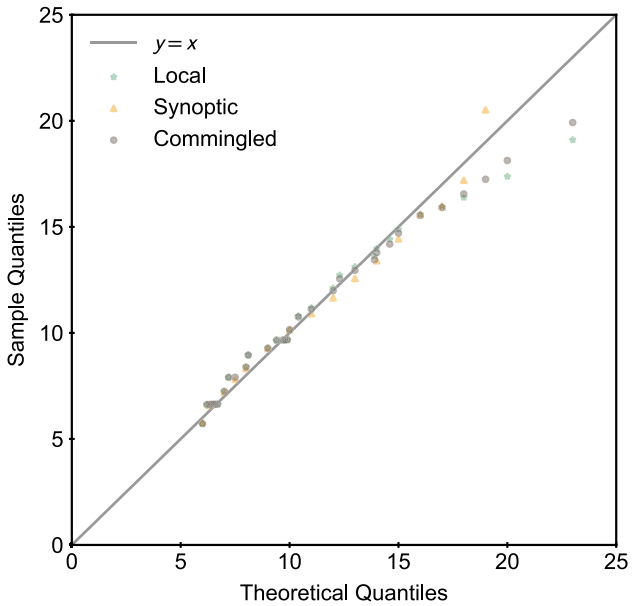

Fig. 19 Q–Q plot of the Gumbel distribution fitting different extreme wind speed sample at DAWU

distribution. Murong synoptic wind distribution shape is very similar with Fig. 17. The annual exceed probability of synoptic wind $P_S(u \leq U)$ is calculated by Eq. (3) by $T = 1$.

Extreme wind speed of different type wind events and mixture climate could be calculated by Eq. (7). The calculation result is shown in Fig. 24. The mixed line is the envelope of the extreme wind speed of the local wind system and synoptic wind system.

"Commingled line" stands for the results from MIS without sorted windspeed data, which contains few synoptic wind. So it is very closed to "Local line". In order to consider the synoptic wind effect on Murong, the synoptic wind speed record at DAWU is used by maximum wind speed transferring. As shown in Fig. 24, "synoptic line" has a larger slope compared to "local line". In mountainous areas, the extreme wind speeds of long and short return periods are determined by different wind systems. For short

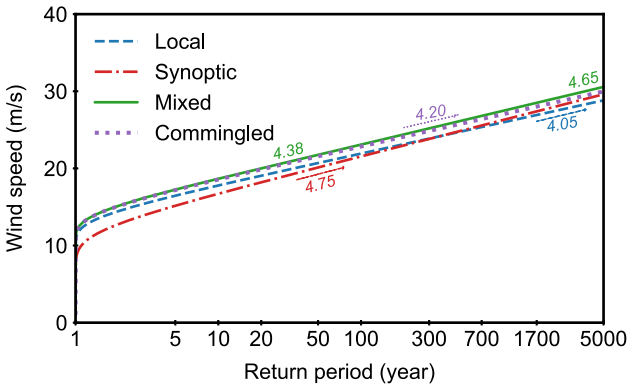

Fig. 20 Extreme wind speed of different return period at DAWU

Table 3 Estimated parameter values and quantitative performance of local wind speed parent sample fitted by the Weibull distribution

Distribution type	Estimated parameter values			Performance	
	Location	Scale	Shape	AIC	BIC
Weibull	0.011	3.229	1.189	139121	139146

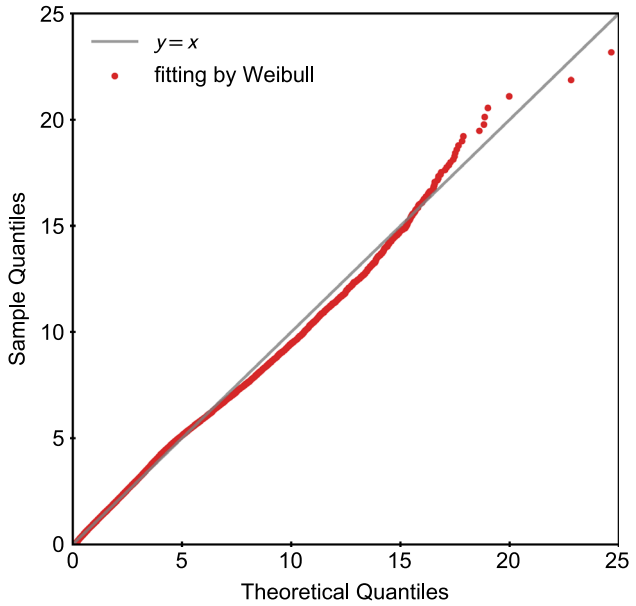

Fig. 21 Q–Q plot of the Weibull distribution fitting local wind speed parent sample

return period, local wind system is more important. On the contrary, it is the synoptic wind system that plays a dominating role for long return period. The extreme wind speed will be underestimated without sorted data and synoptic wind augmentation, especially for long return period.

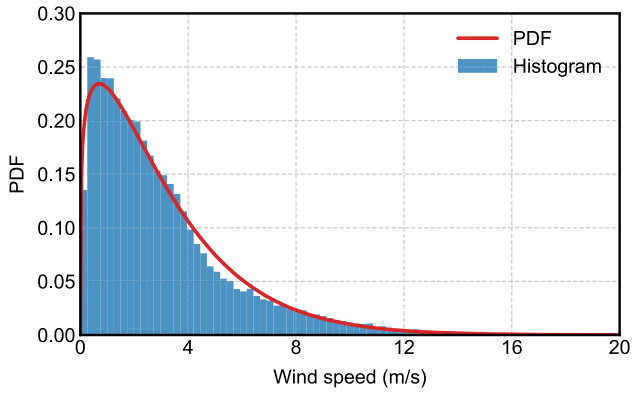

Fig. 22 Distribution of wind speed parent population at Murong, empirical histogram and PDF model (Weibull)

6 Discussion

Extreme data need to be sorted according to the different wind producing weather systems before carrying out any analyses, as suggested by Gomes and Vickery (1977, 1978). Sorting is needed since the wind that is generated by the different weather systems has different characteristics and probability of occurrences (Choi and Tanurdjaja 2002). In this section, how mountainous mixed wind climate influence the extreme wind speed will be discussed.

Extreme wind speed in mixed climate is a historical topic since 1970s. First interest of mixed wind climate system is thunderstorm. Lots of scholars focus on how thunderstorm control the extreme wind speed prediction value of different return periods in different places, such as Australia (Gomes and Vickery 1978), Melbourne (Holmes 2007), West Texas (Twisdale and Vickery 1992) and New York (Lombardo et al. 2009). Choi and Tanurdjaja (2002) proposed that mixed wind climate in Singapore should be divided into large- and small-scale wind systems. Most of those researches show that gathering the ensemble of all the extremes into a single set leads to underestimating the extreme peak wind speed especially for high return periods. Mountainous mixed wind system is firstly discussed in this work. This section will discuss how the mountainous wind system influence the extreme wind speed by sorting into local and synoptic wind system.

Compared with the traditional method which do not distinguish different wind systems, mountainous extreme wind speed shows a similar conclusion to other studies. Firstly, results from the DAWU station show the influence of mountainous mixed wind climate on extreme wind speed. The way of extreme wind speed calculation and distribution types of sample are totally the same. The only difference between mixed and commingled curves is that one distinguishes samples and the other is not. The results

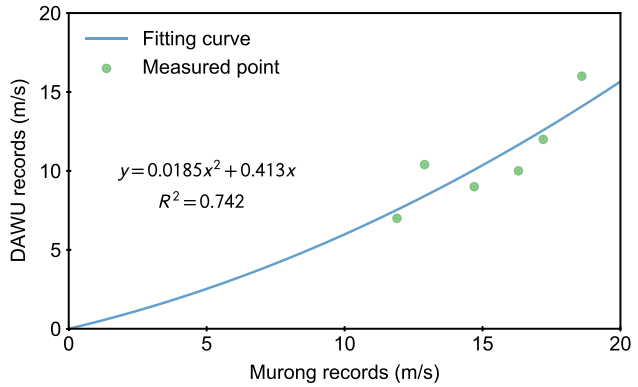

Fig. 23 Maximum wind speed of synoptic wind event mapping relationship between Murong and DAWU

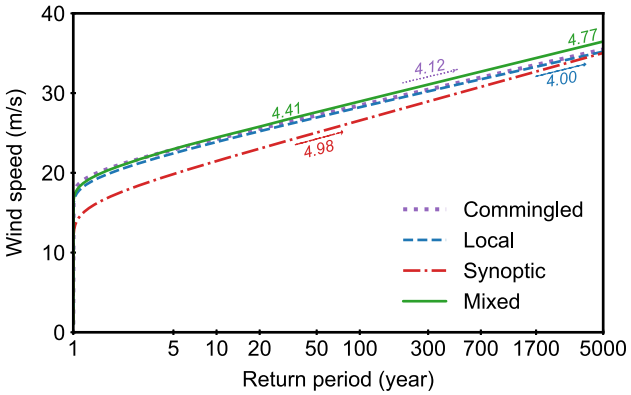

Fig. 24 Extreme wind speed of different return period at Murong

show only a slight difference between those of the mixed and commingled curves. Non-sorted wind speed data (commingled curve) underestimates mountainous extreme wind speeds during high return periods. This slight difference is likely due to the characteristics of the local and synoptic wind systems in mountain.

7 Conclusion

This paper presents a novel method for mountainous extreme wind speed calculation with a focus on mountainous mixture wind system composed of local wind system and synoptic wind system. This method can be separated into three parts. First, each wind event sub-sequence are extracted by feature points and iterative searching from the wind speed raw data and classified into local wind and synoptic wind. Second, the mapping relationship on maximum wind speed of synoptic wind system between meteorological observatory and target site is established. And it is used to increase the sample size of synoptic wind events. Third, the annual wind speed exceeding probability of the local wind system and synoptic wind system are calculated by uncrossing rate and method of independent storm respectively. At last, different return period extreme wind speed could be calculated. The difficulty in calculating extreme wind speed in mountainous areas is the limited amount effective field measurement wind speed data. This method extracts synoptic wind event which is the effective information for target site extreme wind speed from surrounding meteorological observatory based on the different characteristics of mountain wind system. Therefore, the calculation of extreme wind speed in mountainous areas could be cheap and accurate.

Murong bridge site is an application in this research which is located in a canyon on western China. In order to calculate the extreme wind speed in Murong, this work uses 10 months of field-measured data and 30 years of wind speed data from the DAWU weather station which is 70 km away from Murong. The calculation results prove that the extreme wind speed in the short return period is controlled by the local wind system, and synoptic wind system plays a decisive role on long return period extreme wind speed.

Author Contributions Conceptualization: CW, MT; Methodology: MT; Formal analysis and investigation: MT, CW; Data curation: WC, YD; Writing - origin draft preparation: MT; Writing - review and editing: CW, ZL; Funding acquisition: CW, ZL; Supervision: GF, ZL, GY.

Funding The authors gratefully acknowledge the support of National Natural Science Foundation of China (52078383, 52008314) and Independent subject of State Key Lab of Disaster Reduction in Civil Engineering (SLDRCE19-B-11).

Declarations

Conflict of interest All authors certify that they have no affiliations with or involvement in any organization or entity with any financial interest or non-financial interest in the subject matter or materials discussed in this manuscript.

References

Abd-Elaal ES, Mills JE, Ma X (2018) Numerical simulation of downburst wind flow over real topography. J Wind Eng Ind Aerodyn 172:85–95

ASCE (2016) Minimum design loads for building and other structures (ASCE 7-16)

Beine H, Argentini S, Maurizi A et al (2001) The local wind field at ny-å lesund and the zeppelin mountain at svalbard. Meteorol Atmos Phys 78(1):107–113

Bitsuamlak G, Stathopoulos T, Bedard C (2004) Numerical evaluation of wind flow over complex terrain. J Aerosp Eng 17(4):135–145

Cao S, Wang T, Ge Y et al (2012) Numerical study on turbulent boundary layers over two-dimensional hills-effects of surface roughness and slope. J Wind Eng Ind Aerodyn 104:342–349
Chen G, Lombardo FT (2020) An automated classification method of thunderstorm and non-thunderstorm wind data based on a convolutional neural network. J Wind Eng Ind Aerodyn 207(104):407
Choi E, Tanurdjaja A (2002) Extreme wind studies in singapore an area with mixed weather system. J Wind Eng Ind Aerodyn 90(12–15):1611–1630
Cook N (1982) Towards better estimation of extreme winds. J Wind Eng Ind Aerodyn 9(3):295–323
Cook NJ (2004) Confidence limits for extreme wind speeds in mixed climates. J Wind Eng Ind Aerodyn 92(1):41–51
Cook NJ, Harris RI, Whiting R (2003) Extreme wind speeds in mixed climates revisited. J Wind Eng Ind Aerodyn 91(3):403–422
Cui W, Caracoglia L (2020) Performance-based wind engineering of tall buildings examining life-cycle downtime and multisource wind damage. J Struct Eng 146(1):04019,179
Cui W, Ma T, Zhao L et al (2021) Data-based windstorm type identification algorithm and extreme wind speed prediction. J Struct Eng 147(5):04021,053
De Gaetano P, Repetto MP, Repetto T et al (2014) Separation and classification of extreme wind events from anemometric records. J Wind Eng Ind Aerodyn 126:132–143
Deng H, Runger G, Tuv E et al (2013) A time series forest for classification and feature extraction. Inf Sci 239:142–153
Fisher RA, Tippett LHC (1928) Limiting forms of the frequency distribution of the largest or smallest member of a sample. In: Mathematical proceedings of the Cambridge philosophical society, Cambridge University Press, pp 180–190
Fulcher BD, Jones NS (2014) Highly comparative feature-based time-series classification. IEEE Trans Knowl Data Eng 26(12):3026–3037
Gaidai O, Naess A, Xu X et al (2019) Improving extreme wind speed prediction based on a short data sample, using a highly correlated long data sample. J Wind Eng Ind Aerodyn 188:102–109
Gomes L, Vickery B (1977) On the prediction of extreme wind speeds from the parent distribution. J Wind Eng Ind Aerodyn 2(1):21–36
Gomes L, Vickery B (1978) Extreme wind speeds in mixed wind climates. J Wind Eng Ind Aerodyn 2(4):331–344
Gumbel EJ (2004) Statistics of extremes. Courier Corporation
Harris R (1999) Improvements to themethod of independent storms'. J Wind Eng Ind Aerodyn 80(1–2):1–30
Holmes JD (2007) Wind loading of structures. CRC Press, Boca Raton
van der Hoven I (1957) Power spectrum of horizontal wind speed in the frequency range from 0.0007 to 900 cycles per hour. J Atmos Sci 14(2):160–164
Huang G, Jiang Y, Peng L et al (2019) Characteristics of intense winds in mountain area based on field measurement: focusing on thunderstorm winds. J Wind Eng Ind Aerodyn 190:166–182
Jackson PL, Mayr G, Vosper S (2013) Dynamically-driven winds. Mountain weather research and forecasting. Springer, Berlin, pp 121–218
Jing H, Liao H, Ma C et al (2020) Field measurement study of wind characteristics at different measuring positions in a mountainous valley. Exp Thermal Fluid Sci 112(109):991
Kim HG, Patel V, Lee CM (2000) Numerical simulation of wind flow over hilly terrain. J Wind Eng Ind Aerodyn 87(1):45–60
Kwok KC, Hitchcock PA, Burton MD (2009) Perception of vibration and occupant comfort in wind-excited tall buildings. J Wind Eng Ind Aerodyn 97(7–8):368–380
Li C, Chen Z, Zhang Z et al (2010) Wind tunnel modeling of flow over mountainous valley terrain. Wind Struct 13(3):275
Li Y, Zhang M, Xu X et al (2014) Causes of daily strong wind on bridge site in deep gorge with high altitude and high temperature difference. J Southwest Jiaotong Univ 49(6):935–941
Li Y, Xu X, Zhang M et al (2017) Wind tunnel test and numerical simulation of wind characteristics at a bridge site in mountainous terrain. Adv Struct Eng 20(8):1223–1231
Lombardo FT, Main JA, Simiu E (2009) Automated extraction and classification of thunderstorm and non-thunderstorm wind data for extreme-value analysis. J Wind Eng Ind Aerodyn 97(3–4):120–131
Maurizi A, Palma J, Castro F (1998) Numerical simulation of the atmospheric flow in a mountainous region of the north of portugal. J Wind Eng Ind Aerodyn 74:219–228
Mingjin Z, Jisheng Y, Jingyu Z et al (2019) Study on the wind-field characteristics over a bridge site due to the shielding effects of mountains in a deep gorge via numerical simulation. Adv Struct Eng 22(14):3055–3065
Palutikof J, Brabson B, Lister D et al (1999) A review of methods to calculate extreme wind speeds. Meteorol Appl J Forecast Pract Appl Train Tech Modell 6(2):119–132
Pavan M, Mizzaro S, Scagnetto I (2017) Mining movement data to extract personal points of interest: a feature based approach. Information filtering and retrieval. Springer, Berlin, pp 35–61
Ren H, Laima S, Chen WL et al (2018) Numerical simulation and prediction of spatial wind field under complex terrain. J Wind Eng Ind Aerodyn 180:49–65
Rice SO (1944) Mathematical analysis of random noise. Bell Syst Tech J 23(3):282–332
Simiu E, Heckert N (1996) Extreme wind distribution tails: a peaks over threshold approach. J Struct Eng 122(5):539–547
Simiu E, Yeo D (2019) Wind effects on structures: modern structural design for wind. John Wiley and Sons, New Jersey
Simo-Serra E, Trulls E, Ferraz L, et al (2015) Discriminative learning of deep convolutional feature point descriptors. In: Proceedings of the IEEE international conference on computer vision, pp 118–126
Tongji-University (2018) Wind-resistant design specification for highway bridges (JTG/T 3360-01-2018)
Tse KT, Weerasuriya AU, Hu G (2020) Integrating topography-modified wind flows into structural and environmental wind engineering applications. J Wind Eng Ind Aerodyn 204(104):270
Twisdale LA, Vickery PJ (1992) Research on thunderstorm wind design parameters. J Wind Eng Ind Aerodyn 41(1–3):545–556
Wagner A (1938) Theorie und beobachtung der periodischen gebirgswinde (theory and observation of periodic mountain winds). Gerlands Beitr Geophys 52:408–449
Wang Q (2001) A bayesian joint probability approach for flood record augmentation. Water Resour Res 37(6):1707–1712
Whiteman CD (1990) Observations of thermally developed wind systems in mountainous terrain. Atmospheric processes over complex terrain. Springer, Berlin, pp 5–42
Young AH, Knapp KR, Inamdar A et al (2018) The international satellite cloud climatology project h-series climate data record product. Earth Syst Sci Data 10(1):583–593
Zardi D, Whiteman CD (2013) Diurnal mountain wind systems. Mountain weather research and forecasting, pp 35–119
Zhang J, Zhang M, Li Y et al (2020) Comparison of wind characteristics at different heights of deep-cut canyon based on field measurement. Adv Struct Eng 23(2):219–233
Zhang M, Zhang J, Li Y et al (2020) Wind characteristics in the high-altitude difference at bridge site by wind tunnel tests. Wind Struct 30(6):547–558
Zhao J, Itti L (2015) Classifying time series using local descriptors with hybrid sampling. IEEE Trans Knowl Data Eng 28(3):623–637